DR. MICHAEL HENEKA (Orcid ID : 0000-0003-4996-1630)

Article type : Original Article

Microglia modulation through external vagus nerve stimulation in a murine model of Alzheimer's disease

Robert Kaczmarczyk[1], Dario Tejera[1], Bruce J. Simon[2], Michael T. Heneka[1]

[1]Department of Neurodegenerative Disease and Gerontopsychiatry, University of Bonn, Bonn Germany

[2]electroCore LLC, Basking Ridge, New Jersey, U.S.A.

Correspondence to:

Michael T. Heneka, MD

Dept. of Neurodegenerative Disease and Gerontopsychiatry

Sigmund-Freud Str. 25

53127 Bonn

Germany

(p) +49 228 28713091

(f) +49 228713166

(e) michael.heneka@ukb.uni-bonn.de

List fo abbreviations

AD - Alzheimer's disease

Ach - acetylcholine

NE - norepinephrine

VNS - Vagus nerve stimulation

nVNS - Non-invasive vagus nerve stimulation

This article has been accepted for publication and undergone full peer review but has not been through the copyediting, typesetting, pagination and proofreading process, which may lead to differences between this version and the Version of Record. Please cite this article as doi: 10.1111/jnc.14284

iVNS - invasive vagus nerve stimulation

LC - locus coeruleus

Aβ - β-amyloid deposits

NBM - Nucleus Basalis of Meynert

HPLC - high-performance liquid chromatography

2PLSM - 2-photon laser scanning in vivo microscopy

CAP - cholinergic anti-inflammatory pathway

DSP-4 - N-(2-chloroethyl)-N-ethyl-2-bromobenzylamine

MLA - methyllycaconitine

APP - Amyloid precursor protein

PS-1 - Presenilin-1

mvt - multivariate t distribution

Abstract

Chronically activated microglia contribute to the development of neurodegenerative diseases such as Alzheimer's disease (AD) by the release of proinflammatory mediators that compromise neuronal function and structure.. Modulating microglia functions could be instrumental to interfere with disease pathogenesis.. Previous studies have shown an anti-inflammatory effects of acetylcholine (ACh) or norepinephrine (NE), which mainly activate the β-receptors on microglial cells. Non-invasive vagus nerve stimulation (nVNS) is used in treatment of drug resistant depression, which is a risk factor for developing AD. The vagus nerve projects to the brainstem's locus coeruleus (LC) from which noradrenergic fibers reach to the Nucleus Basalis of Meynert (NBM) and widely throughout the brain. Pilot studies showed first signs of cognitive-enhancing effects of nVNS in AD patients. In the present study, the effects of nVNS on mouse microglia cell morphology were analysed over a period of 280 minutes by 2-photon laser scanning in-vivo microscopy. Total branch length, average branch order and number of branches, which are commonly used indicators for the microglial activation state were determined and compared between young and old wild-type and APP/PS1 transgenic mice. Overall, these experiments show strong morphological changes in microglia, from a neurodestructive to a neuroprotective phenotype, following a brief nVNS in aged animals, especially in APP/PS1 animals, while microglia from young animals were morphologically unaffected.

Introduction

Alzheimer's disease (AD) is the most common cause of dementia in the elderly, affecting about 1/3 of people at or over the age of 85, currently affecting 31 million patients worldwide (Association and others 2017). The underlying causes of AD remain elusive to date, but associations have been found between β-amyloid deposits (Aβ), neurofibrillary tangle formation, neuroinflammation and disease progression. As age is the main risk factor for AD, the large aging population will lead to even higher numbers of people suffering from AD in the near future (Kandel 2013). Therefore, understanding disease pathogenesis and finding new treatments for AD is of utmost importance. The locus coeruleus (LC) is an aminergic brain stem nucleus, which is located at the tegmentum of the 4th ventricle, and represents the main source of norepinephrine (NE) in the brain. Axons project from there into all brain areas, with the neocortex and hippocampus receiving the major part of these projections. Physiologically, LC-derived NE plays a vital role in arousal, attention, learning and behavioural adaptation. In addition to its role as a classical neurotransmitter, NE also functions as an immune modulator, inducing the neuroprotective action of microglia and suppressing the detrimental release of pro-inflammatory mediators (Jardanhazi-Kurutz *et al.* 2010; Jardanhazi-Kurutz *et al.* 2011). The LC suffers from declining cell numbers in aged mammalian brains, but the loss of LC neurons is even greater in AD patients. LC neuron loss correlates with neurofibrillary tangle load, Aβ plaque deposition, and the severity of dementia (Bondareff *et al.* 1987). Loss of LC neurons correlates better with the progression of AD than the degeneration of the Nucleus Basalis of Meynert (NBM), which is a cholinergic nucleus and commonly associated with AD pathology (Förstl *et al.* 1994; Zarow *et al.* 2003). Experimentally induced LC degeneration and subsequent decline of NE levels in its projection areas resulted in increased microglial and astrocyte immune activation, compromised microglial phagocytosis and clearance of Aβ (Jardanhazi-Kurutz *et al.* 2010; Jardanhazi-Kurutz *et al.* 2011; Heneka *et al.* 2010; Kalinin *et al.* 2007). A key feature of microglial activation in response to pathological stimuli is process retraction and overall reduction of process length. In addition, the cell soma volume increases and the overall shape of the cell becomes oval. In this state, physiological microglial functions, including surveillance and removal of debris, are strongly compromised due to the overall reduction of the environmental space scanned by the individual cell (Ransohoff 2016). Pharmacologically, elevation of cerebral NE levels by treatment of rodents with the NE precursor L-threo-DOPS allows resetting of microglial key functions such as migration and Aβ phagocytosis (Heneka *et al.* 2010). Vagus nerve stimulation (VNS) has been shown to increase NE (Hassert *et al.* 2004; Follesa *et al.* 2007; Raedt *et al.* 2011; Roosevelt *et al.* 2006) in the brain within minutes after stimulation, as measured by high-performance liquid chromatography (HPLC). Furthermore, different anatomical studies have shown that VNS also activates the central cholinergic

system (Hulsey *et al.* 2016; Hays 2016; Smiley *et al.* 1999) and its efficacy is reduced when scopolamine is used to block muscarinic receptors (Nichols *et al.* 2011). Direct increase of ACh brain levels following VNS remains to be explored in further animal studies though. Moreover, the increase in these neurotransmitters caused a reduction in cytokine secretion in macrophages and T-cells (Rosas-Ballina *et al.* 2011; Vida *et al.* 2011). Additionally, it was shown that an intact LC (Krahl *et al.* 1998; Grimonprez *et al.* 2015) and NBM (Hulsey *et al.* 2016) is required for the nVNS effect confirming that not only NE but also ACh plays an important role in the mechanism of nVNS.

Therefore, the present study assessed whether such a nonpharmacological intervention would be able to revert the morphological signs of microglial activation in a murine AD model. Wild-type (WT) and APP/PS1 transgenic animals, also expressing CX3CR1-EGFP to visualize brain microglia, were analyzed by 2-photon laser scanning in vivo microscopy (2PLSM), allowing an assessment of dynamic cellular changes in a longitudinal manner. Mice were investigated at 6 and 12 months of age, to determine age-dependent and disease-related changes. Dynamic morphological changes were recorded at identical positions over time and the number of branches, total branch length and the average branch order were analyzed.

Materials and methods

Materials

Gelita Tampon (B. Braun, REF 2070600), Sugi (Kettenbach, REF 30601), Technikmaster C2/SF (Schick, REF A764859), Driller (Komet dental Gebr. Brasseler, REF H71104004), Cyano Fast glue (Hager Werken, REF 152261), Harvard Implant semi-permanent cement (Harvard Dental International GmbH, REF 7081400), Xylocaine liquid (Lidocaine 2% with epinephrine 1:100,000 solution, Dentsply GmbH, REF 198554863), Isoflurane (Piramal, 250ml, REF 30372), Venus Flow (Heraeus Kulzer, REF 66014561), Ketamin (Ratiopharm GmbH, 50 mg/ml, REF 7538837), Xylazine 2% 1 (Serumwerk Bernburg AG, REF 04-03-9267/22), 0,9% NaCl (Fresenius Kabi, REF 00809090), Buprenorphine (Temgesic, Indivior, REF 3015552), Dexamethasone (Jenapharm®, 6mg/ml, REF 08704344), Cefotaxim (Ratiopharm, REF 109697.03), Octenisept (Schülke & Mayr GmbH, REF 104012), Head Holding Adaptor for Mice MA6N (Narishige), eye ointment (Bepanthen, Bayer, 5g, REF 02182442), VEET® depilatory cream, Carprofen (Rimadyl®, Pfizer GmbH, 50 mg/ml, REF 054594), feather disposable scalpel No 11 (Feather®, REF 0200130011)

Animals

Six- and 12-month-old double transgenic mice hemizygous for a chimeric mouse/human amyloid precursor protein and a mutant human presenilin 1 (PS1-ΔE9; PS1) protein as well as for a green fluorescent protein expressed under a CX3CR1 promoter were used (APP/PS1[+/-]/CX3CR1-EGFP[+/-]). The control groups consisted of 6 and 12 month-old CX3CR1-EGFP[+/-] transgenic mice which weighted between 28 and 43 grams each. Animals were housed and mated in our animal facility in groups of four at a 12 h light/dark cycle and a temperature of 22°C with ad libitum access to standard food and water. The study was preregistered, animal care was approved by the local ethics committee (AZ: 84-02.04.2013.A101).

Cranial window placement

A cranial window was placed into the right hemisphere and fixed with a titanium ring for stable 2PLSM image-acquisition as previously described (Hefendehl et al. 2012; Holtmaat et al. 2009). Mice received an intraperitoneal injection (i.p.) of ketamine/xylazine (0.13/0.01 mg/g body weight), followed by subcutaneous injections (s.c.) of buprenorphine (10 µl/10 g body weight), dexamethasone (10 µl/10 g body weight) and cefotaxime (10 µl/10 g body weight). Bepanthene eye ointment was applied to the eyes to avoid drying. The surgical instruments were sterilized in a bead heater (CellPoint Scientific Inc., Germinator™ 500). The hair was removed using VEET® depilatory cream. The mouse was then put into a stereotactic frame and antiseptic was applied on the skin of the head. The disinfected skin was then removed using sharp scissors. One drop of 2% xylocaine and 1:100,000 epinephrine solution was applied both to the periosteum and the uncovered muscles. The periosteum was then removed by gently scraping with a scalpel to increase the gluing capacity between the ring and the skull. A wall of cyanoacrylate was prepared around the location and a 4 mm diameter hole was carefully drilled over the right hemisphere in a parietal position using a Schick C2 drilling device at ~25,000 rpm next to the sagittal suture. The drilling device was constantly cooled with a 154 mmol/l sodium chloride solution. The loose bone was gently removed with sharp forceps. Venus flow glue was put onto a small needle and applied around the drilled hole at a distance of 1 mm to avoid touching the dura. A 5 mm coverslip was put on top. Subsequently, the coverslip was pressed with forceps to achieve the smallest brain to coverslip distance possible, followed by exposure to ultraviolet light for 30 seconds to harden the glue. Next the edges of the coverslip were fixed by putting cyanoacrylate on the bottom part of a custom-made titanium ring, which was placed on the head. The outer parts were attached to the skull using Harvard semi-implant cement. After the operation, the mouse was put under infrared light for recovery. The body temperature was controlled throughout the procedure and maintained at 37°C. Implantation of the cranial window was trained at different laboratories in Germany specialized in cranial window

operations (Institutes of Physiology in Bonn and in Tübingen). We performed a repeated measures analysis to minimize the number of animals needed. Anesthetics and opioids as well as non-steroidal anti-rheumatics were used to reduce animal pain during and after surgery. nVNS was performed under isoflurane anesthesia

In vivo 2PLSM imaging

A Ti:Saphire two-photon-laser-scanning-microscope was used with a Nikon water-immersion objective (25x, 1,10W) and Nikon NIS Elements AR 4.20.03 (Build 995). Imaging was performed under general volatile isoflurane anesthesia (1.2 - 1.5%, flow ˜750ml/min). No randomization were performed, the mice were arbitrary asigned for the treatment, and every day animals from each treatment groups were used for the imaging and analysis. However, the experimenter was blinded for the treatment of the mice. The hair at the right side of the neck was removed using VEET® depilatory cream for later application of nVNS or sham-treatment. The mouse was put onto a heating blanket and rectal temperature was kept constant at 37°C. All images were taken using 925nm for EGFP. An overview image was taken to help with orientation, before three zoomed areas of interest (AOI) were randomly chosen and their positions saved within the Nikon NIS Elements software. The acquired stacks in 300 µm depth consisted of 81 slices covering 120 µm * 120 µm * 40 µm (x*y*z) and 0.5 µm z-space between two adjacent slices. Three stacks per time frame were taken, resulting in a total of 21 stacks. The images were acquired under 4x line averaging technique and x4.348 scanner zoom. The voxel matrix was 512 x 512 x 40 pixels and the voxel size 0.234 µm/pixel. After imaging, the mouse was put back into a heated cage under infrared-light.

Non-invasive Vagus nerve stimulation (nVNS)

After 80 minutes of recording and establishing two baseline stacks of three different regions, nVNS or sham-treatment was performed by applying electrolyte gel (Signa gel; Parker Laboratories, Inc., Fairfield, NJ) onto the stimulator's electrodes. nVNS was performed 13mm anterior to the neck's base and 2mm from the trachea over the vagus nerve (Suppl. Figure 1) similar to the placement position in rats (Ay *et al.* 2016; Oshinsky *et al.* 2014). Using the same signal and a similar protocol as used in previous VNS animal studies (Ay *et al.* 2016; Oshinsky *et al.* 2014), the mouse was stimulated twice for two minutes with a three-minute break in between. The nVNS signal consisted of 1 ms duration bursts of 5 kHz sine waves, repeated at 25

Hz. The signal amplitude was increased until there was strong muscle stimulation, corresponding to approximately 1.8 mA. After the stimulation or sham-treatment, the same three regions were imaged another five times. Sham treatment was performed in the same manner as the nVNS only without turning on the stimulator.

Quantification of morphological cell parameters

Bitplane Imaris v8.1.2 [Jun 3 2015] Build 36825 was used to create a three-dimensional automatic reconstruction of the acquired stacks (Suppl. Figure 2). The following recommended automatic reconstruction settings by Imaris were used: Autopath (no loops), largest branch diameter: 11.7µm, thinnest branch diameter: 0.704µm, diameter of sphere region(s): 23.5µm, automatic starting points threshold and automatic seed points threshold. The number and position of starting points (=microglia cell bodies) was kept constant within the seven timeframes of one region. The parameters for number of branches, total branch length and average branch order were then exported as an excel-file and further analyzed.

Statistical analysis

The R statistical software package (R Core Team 2016) was used to perform a linear mixed effects model analysis, as seven repeated measures from a single mouse were obtained with varying numbers of microglial cells, ranging from n = 31 to 76. (Suppl. Figure 3). Since we did not have information about the predicted variables the sample size was not calculated before. The random effect with random intercept was mouse to account for inter-individual variation, and as fixed effects we used time (per 40 minutes, time-frames 1 to 7), treatment (factor of 2: nVNS or sham treatment), age (factor of 2: 6 months or 12 months) and genotype (factor of 2: APP/PS1[+/-]/CX3CR1-EGFP[+/-] or CX3CR1-EGFP[+/-]). Next, the nlme package (Pinheiro *et al.* 2017) was used to fit our linear mixed effects model and the lsmeans package (Lenth 2016) to compare the least squares means between different groups. The model was fit using maximized log-likelihood. The family wise error rate was taken into account and p-values, standard errors and confidence intervals were adjusted for multiple comparisons (see tables for adjustment-methods). Note that our response variables were square-rooted for the analysis to account for heteroscedasticity (Suppl. Figure 4) and then back-transformed after calculating the least squares means. Therefore, all means, standard errors and confidence intervals were averaged over the 7 observations or 280 minutes in each group. In addition to the square root transformation, we used the weights argument in the lme-function to define the within-group heteroscedasticity structure. Tables 1, 2 and 3 contain multiplicity adjusted p-values and confidence intervals. To

produce “exact” Tukey adjustment (Lenth 2016), multivariate t distribution (mvt) and a Monte Carlo method (Genz and Bretz 2002) were used. To attain reproducible results, the random-number seed within R was set to 0. The data is expressed as mean +/- SEM.

Results

It is widely accepted that microglia, observed in age or chronic inflammation, show fewer and shorter branches compared to physiologically ramified microglia that are usually present in the healthy CNS. We used a linear mixed effects model to analyze the interactions of the four factors time, genotype, age and stimulation on the response variables, total branch length, number of branches and the average branch order, which are parameters that describe the ramification of microglial cells. The data predict an age- ($p = 0.044$) and stimulation-dependent morphological change ($p = 0.001$) over time. In addition, the effects of nVNS were slightly but significantly ($p = 0.024$) different between the young and old animals. The data suggest no genotype-related morphological changes over time (Suppl. Table 1). Before the nVNS-induced changes of microglial morphology were elaborated, the changes between age- or genotype-matched groups were assessed, as non-nVNS-related alterations would make any further interpretation more challenging. The obtained data revealed no significant differences for time-dependent morphology changes for all three response variables across all groups (Suppl. Tables 2). Next, we assessed the microglial morphology in age- and genotype-matched groups and compared nVNS mice with sham treated controls. The nVNS or sham treatment was performed 80 minutes after starting in vivo 2PLSM, enabling the detection of differences of morphology dynamics upon nVNS during the subsequent 200 minutes of image acquisition. Each time point in the diagrams represents a time-frame of 40 minutes, e.g. 160 minutes is the period between 160 and 200 minutes of image acquisition. We calculated least squares means of the trends and compared stimulated with sham treated mice within age- and genotype matched groups. The differences of the slopes of the linear regression lines (Figure 1 and Suppl. Figure 5: dotted lines in C, D and E) of nVNS and sham treated mice were calculated and analyzed. nVNS in 12-month-old APP/PS1 mice caused a significant difference in the time-dependent changes of branch number ($p < 0.001$) compared to sham treated littermates, increasing the difference in number of branches between nVNS and sham treated controls by 3.82 +/- 0.90 branches every 40 minutes. There was a non-significant trend for 12-month-old WT mice ($p = 0.071$; Figure 1 C and F) in which the difference in branch number increased by 2.07 +/- 0.88 every 40 minutes (Table 1). nVNS stimulation in both 6-month-old groups showed no difference (Suppl. Figure 5 C and F; Table 1). Alterations in microglial morphology were further assessed by dynamic recording of total branch length in the

3D microglia reconstructions. Again, the 12-month-old APP/PS1 groups had a significant difference in total branch length dynamics ($p < 0.01$; Figure 1 D and G), with an increasing difference of the total branch length between nVNS and sham treated mice of 41.77 µm +/- 12.31 µm (Table 2). Correspondingly, the 12-month-old WT animals had a similar non-significant trend ($p = 0.091$; Figure 1 D and G), where the average difference between nVNS and sham treated mice increased by 30.82 µm +/- 13.61 µm in total branch length every 40 minutes (Table 2). The young animals showed no difference between stimulated and sham treated mice (Table 2). Average branch order is a parameter for measuring branching tree complexity and is usually associated with surveying healthy microglia. In contrast to the results obtained for branch number and total branch length, a significant difference in the average branch order dynamics between stimulated and sham-treated mice ($p < 0.05$; Figure 1 E and H) became apparent in the WT 12-month-old group, where the difference in branch order between the nVNS and sham treated group increased by 0.64 +/- 0.25 every 40 minutes (Table 3). The 12-month-old APP/PS1 group had a non-significant trend ($p = 0.0897$, Figure 1 E and H) towards increasing the difference in branch order by 0.47 +/- 0.21 every 40 minutes (Table 3). No differences were found between stimulated and sham-treated mice in the 6-month-old groups (Table 3).

Discussion

Microglia cells represent a key part of the brain's innate immune system and are involved in several physiological and pathophysiological processes aimed at the maintenance of brain homeostasis and integrity throughout our lives. These cells show a distinct morphology with multiple processes and branches, which enable them to scan and survey their immediate environment (Ransohoff 2016). Multiple contacts are constantly made between neurons and microglia, e.g. during early development to prune and scale synaptic contacts (Miyamoto *et al.* 2013). However, during aging and moreover in response to pathological processes, these cells undergo fundamental changes resulting in process retraction and reduction of branch numbers (Hoeijmakers *et al.* 2016). In this study, morphological changes of microglia were analyzed in wild type and APP/PS1 transgenic mice, a murine model of AD, by two photon laser scanning live microscopy. Moreover, the effects of nVNS were measured longitudinally in both conditions. The results of this study suggest that morphological signs of microglial aging and activation can be reversed by nVNS.

Physiological aging is associated with immune senescence, which is reflected in the brain by a switch from a resting, surveying to an activated microglial phenotype. Healthy microglial cells do not only have better A*β* phagocytosis capabilities, but also release neurotrophic factors, e.g. BDNF and

bFGF, and anti-inflammatory cytokines such as IL-4, IL-10 and TGFβ. Activated microglial cells on the other hand release pro-inflammatory cytokines, e.g. IL-1β, IL-6 and TNFα, and have reduced Aβ clearance. Some authors further distinguish between dystrophic microglia as observed in the aging brain and reactive hypertrophic microglia in acute injuries (Ransohoff 2016). Both resemble the activated phenotype with retracted and fewer branches compared to long ramified branches in the healthy state (Ransohoff 2016). Hoeijmakers et al. suggested a two-hit mechanism similar to that seen in tumour pathogenesis: an initial event like a neonatal infection or aging leads to primed microglia which are then susceptible to systemic infection or immune challenges (Hoeijmakers *et al.* 2016). As a consequence, the microglia cells retract their processes and secrete pro-inflammatory cytokines. It is suggested that in the case of AD, increasing Aβ levels lead to a neuroinflammatory environment, resulting in neurotoxicity with subsequent cognitive decline (Ransohoff 2016). For now, the exact chronological order of pathological mechanisms remains elusive.

Our results show that 12-month-old APP/PS1 animals with greater Aβ plaque deposition, benefited more from nVNS than wild type or 6-month-old APP/PS1 animals. A recent paper has demonstrated that the activation of α7 nicotinic acetylcholine receptors (α7nAChR) is able to reverse the LPS-induced microglia conversion to an activated state. This general mechanism is often referred to as the cholinergic anti-inflammatory pathway (CAP) (Zhang *et al.* 2017). It's reasonable to suggest that the microglia phenotype changes seen in this current study might be the result of CAP activation. Previous studies have shown that LC-degeneration precedes that of the NBM in AD patients (Förstl *et al.* 1994; Zarow *et al.* 2003). Moreover, patients with dementia and a history of depression have a significantly greater loss in LC neurons but also a slightly higher NBM neuronal density (Förstl *et al.* 1994). In our case, we assume that in the 12-month-old APP/PS1 animals the immediate response to nVNS, subsequent NBM activation (Hulsey *et al.* 2016) and ACh release alter the morphological phenotype of the microglia cells. The LC also modulates the effect of nVNS – indeed LC neurons project to the NBM and this mechanism of interaction has already been suggested (Heneka *et al.* 2010). A study on trigeminal allodynia in rats showed no significant differences following nVNS in the levels of NE but an increase in glutamate levels in trigeminal nucleus caudalis (TNC) (Oshinsky *et al.* 2014). LC activity however was significantly increased for up to 3 days after nVNS (Dorr and Debonnel 2006), whereas NE levels only persisted during the stimulation-periods (Roosevelt *et al.* 2006). Recently, Hulsey et al. characterized LC activity following VNS (Hulsey *et al.* 2017).

These findings support the hypothesis, that there is a tonic modulatory effect of LC, which does not only rely on NE as a neuromodulator (Figure 2). The 12-month-old WT animals also showed increasing average branch order compared to sham-treated controls. As in our case, the 6-month old mice did not react to nVNS, thus age is a more crucial stimulus for priming microglia than the APP/PS1 phenotype with the early Aβ-deposition. These conclusions are valid under the assumption that primed microglia are more susceptible to nVNS-mediated morphology changes than healthy ramified microglia. Ramified microglia are constantly surveying their environment and secrete neurotrophic factors in a healthy brain, whereas this ability may be lost in primed microglia in the senescent brain, especially in mice expressing the APP/PS1 gene (Daria *et al.* 2017). Our data show for the first time that morphological changes of activated microglia may be directly reversed by nVNS. This mechanism may involve nVNS activation of LC and release of NE since LC degeneration in APP/PS1 mice increases A*β* plaque deposition which triggers microglia priming (Phillips *et al.* 2016). We hypothesize that stimulation of the vagus nerve increases activation of the LC and NBM, which leads to higher levels of NE and ACh, respectively, in the brain, which in turn might account for the reversed microglia phenotype. However, we can not rule out the contribution of other excitatory mechanisms.

nVNS therapeutic range

There are two concerns regarding nVNS and the proposed underlying mode of action. Firstly, the homomeric *α*7nAChR shows rapid desensitization when exposed to high levels of receptor agonists. It can even lead to cytotoxicity in exposure to high levels of ACh in the presence of an allosteric modulator, probably mediated by Ca^{2+} overload (Han *et al.* 2017). Secondly, VNS seems to work best with moderate intensity stimulation compared with lower and higher intensity stimulation during memory enhancing treatment (Hays 2016). The inter-individual differences of skin conductivity or thickness of the fat tissue and the skin make a physiological, molecular or radiological marker for nVNS dependent activation necessary. Recently, MRI (Yakunina *et al.* 2017) has been shown to be a promising method to obtain individually tailored stimulations. In contrast to the anti-inflammatory effects of NE, an inverted-U relationship (Yerkes-Dodson law) is seen between nVNS intensity and cognitive enhancing effects (Hays 2016). A first cognitive enhancing effect of nVNS in AD patients was seen in a pilot study (Sjögren *et al.* 2002) and the one-year follow-up results (Merrill *et al.* 2006). Our focus in this study was to analyze the non-invasive, transcutaneous excitation of the vagus nerve and the subsequent effects on microglia cell morphology. The amplitude of the signal was determined by increasing voltage until moderate muscle contraction was observed as described in previous studies in rat with a similar stimulation (Ay *et al.* 2016; Chen *et al.* 2016). Thus, we cannot

exclude an overstimulating or paralytic effect on the microglia of young mice or activation of other excitable structures. However, the previous studies (Chen *et al.* 2016; Ay *et al.* 2016) compared direct to vagus stimulation with nVNS and found similar results suggesting the same vagus fibers were stimulated.

Microglia, NE, nACh and AD

Under normal conditions, NE helps microglia regulate brain function. Adrenergic *β*1- and *β*2-receptors are the only functionally significant adrenergic receptors in microglia within the cortex and are activated primarily by NE (O'Donnell *et al.* 2012). Interestingly, proliferation is suppressed by *β*2-receptor activation. NE is able to suppress the increase in inflammatory gene expression of microglia (O'Donnell *et al.* 2012) and cortical inflammation in general (Heneka *et al.* 2002; Heneka *et al.* 2003). A persistent activation of microglia on the other hand can lead to a self-regulating cytokine cycle and eventually chronic neuroinflammation (Griffin *et al.* 1998; Campbell 2004). Early anti-neuroinflammatory treatment could prevent microglia from entering this self-regulating pro-inflammatory cytokine cycle, lead to delayed AD progression and in the end, reduce cognitive decline. Anti-neuroinflammatory treatment has to begin early, as neurons are usually irreversibly destroyed in advanced AD (Kandel 2013). Interestingly, only the old animals in the current study showed morphological changes due to nVNS. It is possible that the healthy microglia can't be improved by nVNS, as they already show a surveying, healthy phenotype with long, maximally ramified branches and secrete neurotrophic factors. On the other hand, primed or activated microglia are more susceptible to changes in morphological parameters due to nVNS, as the branching parameters already lie in the bottom end of the scale. Amoeboid, activated phenotype microglia seem to be more susceptible to direct current brain stimulation as they are better equipped with voltage gated ion channels compared with ramified microglia (Gellner *et al.* 2016). Depression, a risk factor for developing AD, is commonly treated with Selective serotonin reuptake inhibitors and Serotonin–norepinephrine reuptake inhibitors which in recent studies revealed an anti-inflammatory modulation of microglial cells (Mourao *et al.* 2016; Dubovický *et al.* 2014; Tynan *et al.* 2012). The interplay between nVNS, LC, NBM and its neurotransmitters remain elusive to this day. However, in a human study using VNS paired with tones to treat chronic tinnitus, patients who were on medication that included a muscarinic antagonist, a norepinephrine agonist, and a Y-amino butyric acid agonist, which could interfere with acetylcholine and norepinephrine release, failed to benefit from VNS (De Ridder *et al.* 2014; Engineer *et al.* 2017). A controversial effect of ATP can be seen in mice following an acute injury, as it causes process retraction in a LPS-activated microglial cell but a process induction in a resting microglial cell (Gyoneva *et al.* 2014). We tried to concentrate

our discussion on the interplay of these components, as many recent papers focus on the immediate effects of ACh without considering chronic, modulating NE effects. Long-term treatment options are more likely to arise from proper balance of both, the modulatory, tonic noradrenergic (O'Donnell *et al.* 2012) and the acute cholinergic anti-inflammatory systems (Han *et al.* 2017) (Figure 2). Future studies using blockers of NE or ACh (e.g. N-(2-chloroethyl)-N-ethyl-2-bromobenzylamine (DSP-4), a selective NE-neurotoxin or methyllycaconitine (MLA) an ACh antagonist), might reveal the mechanism behind nVNS. In the case of epilepsy, previous studies indicate NE as the primary neuromodulator accounting for the protective effects of nVNS, thus suggesting a primary role for LC activation (Roosevelt *et al.* 2006; Vonck *et al.* 2014). The imminent effects on microglia cell morphology seem to be mediated by α7nAChR activation. The morphological responses to nVNS and ACh release in a NE enriched and a NE depleted environment have yet to be explored. Our results give a first glance at a stabilizing effect of nVNS on microglia morphology. We need further studies with transcriptomic and proteomic analysis though to find the exact mechanisms of action behind a potential reversion of activated microglia after nVNS.

```
Involves human subjects:
If yes: Informed consent & ethics approval achieved:
=> if yes, please ensure that the info "Informed consent was achieved for all
subjects, and the experiments were approved by the local ethics committee." is
included in the Methods.

ARRIVE guidelines have been followed:
Yes
=> if No or if it is a Review or Editorial, skip complete sentence => if Yes,
insert "All experiments were conducted in compliance with the ARRIVE
guidelines." unless it is a Review or Editorial

Conflicts of interest:  none
=> if 'none', insert "The authors have no conflict of interest to declare."
=> otherwise insert info unless it is already included

Open Science Badges
=> if yes, please see Comments from the Journal for further information => if
no, no information need to be included in the manuscript
```

Acknowledgments

The authors declare no conflict of interest. The authors would like to thank Professor Emeritus Russell V. Lenth from the Department of Statistics and Actuarial Science of the University of Iowa for the refinement of the lsmeans package according to our needs. This study was supported by the Deutsche Forschung Gemeinschaft (SFB 1089).

References

Association A., others (2017) 2017 Alzheimer's disease facts and figures. *Alzheimers Dement.* **13**, 325–373.

Ay I., Nasser R., Simon B., Ay H. (2016) Transcutaneous Cervical Vagus Nerve Stimulation Ameliorates Acute Ischemic Injury in Rats. *Brain Stimulat.* **9**, 166–173.

Bondareff W., Mountjoy C. Q., Roth M., Rossor M. N., Iversen L. L., Reynolds G. P., Hauser D. L. (1987) Neuronal degeneration in locus ceruleus and cortical correlates of Alzheimer disease. *Alzheimer Dis. Assoc. Disord.* **1**, 256–262.

Campbell A. (2004) Inflammation, neurodegenerative diseases, and environmental exposures. *Ann. N. Y. Acad. Sci.* **1035**, 117–132.

Chen S.-P., Ay I., Morais A. L. de, Qin T., Zheng Y., Sadeghian H., Oka F., Simon B., Eikermann-Haerter K., Ayata C. (2016) Vagus nerve stimulation inhibits cortical spreading depression. *Pain* **157**, 797–805.

Daria A., Colombo A., Llovera G., Hampel H., Willem M., Liesz A., Haass C., Tahirovic S. (2017) Young microglia restore amyloid plaque clearance of aged microglia. *EMBO J.* **36**, 583–603.

De Ridder D., Vanneste S., Engineer N. D., Kilgard M. P. (2014) Safety and efficacy of vagus nerve stimulation paired with tones for the treatment of tinnitus: a case series. *Neuromodulation J. Int. Neuromodulation Soc.* **17**, 170–179.

Dorr A. E., Debonnel G. (2006) Effect of vagus nerve stimulation on serotonergic and noradrenergic transmission. *J. Pharmacol. Exp. Ther.* **318**, 890–898.

Dubovický M., Császár E., Melicherčíková K., Kuniaková M., Račková L. (2014) Modulation of microglial function by the antidepressant drug venlafaxine. *Interdiscip. Toxicol.* **7**.

Engineer C. T., Hays S. A., Kilgard M. P. (2017) Vagus nerve stimulation as a potential adjuvant to behavioral therapy for autism and other neurodevelopmental disorders. *J. Neurodev. Disord.* **9**, 20.

Follesa P., Biggio F., Gorini G., Caria S., Talani G., Dazzi L., Puligheddu M., Marrosu F., Biggio G. (2007) Vagus nerve stimulation increases norepinephrine concentration and the gene expression of BDNF and bFGF in the rat brain. *Brain Res.* **1179**, 28–34.

Förstl H., Levy R., Burns A., Luthert P., Cairns N. (1994) Disproportionate loss of noradrenergic and cholinergic neurons as cause of depression in Alzheimer's disease--a hypothesis. *Pharmacopsychiatry* **27**, 11–15.

Gellner A.-K., Reis J., Fritsch B. (2016) Glia: A Neglected Player in Non-invasive Direct Current Brain Stimulation. *Front. Cell. Neurosci.* **10**, 188.

Genz A., Bretz F. (2002) Comparison of methods for the computation of multivariate t probabilities. *J Comput. Graph Stat.*, 950–971.

Griffin W. S., Sheng J. G., Royston M. C., Gentleman S. M., McKenzie J. E., Graham D. I., Roberts G. W., Mrak R. E. (1998) Glial-neuronal interactions in Alzheimer's disease: the potential role of a "cytokine cycle" in disease progression. *Brain Pathol. Zurich Switz.* **8**, 65–72.

Grimonprez A., Raedt R., Portelli J., Dauwe I., Larsen L. E., Bouckaert C., Delbeke J., et al. (2015) The antidepressant-like effect of vagus nerve stimulation is mediated through the locus coeruleus. *J. Psychiatr. Res.* **68**, 1–7.

Gyoneva S., Davalos D., Biswas D., Swanger S. A., Garnier-Amblard E., Loth F., Akassoglou K., Traynelis S. F. (2014) Systemic inflammation regulates microglial responses to tissue damage in vivo. *Glia* **62**, 1345–1360.

Han B., Li X., Hao J. (2017) The cholinergic anti-inflammatory pathway: An innovative treatment strategy for neurological diseases. *Neurosci. Biobehav. Rev.* **77**, 358–368.

Hassert D. L., Miyashita T., Williams C. L. (2004) The Effects of Peripheral Vagal Nerve Stimulation at a Memory-Modulating Intensity on Norepinephrine Output in the Basolateral Amygdala. *Behav. Neurosci.* **118**, 79–88.

Hays S. A. (2016) Enhancing Rehabilitative Therapies with Vagus Nerve Stimulation. *Neurother. J. Am. Soc. Exp. Neurother.* **13**, 382–394.

Hefendehl J. K., Milford D., Eicke D., Wegenast-Braun B. M., Calhoun M. E., Grathwohl S. A., Jucker M., Liebig C. (2012) Repeatable target localization for long-term in vivo imaging of mice with 2-photon microscopy. *J. Neurosci. Methods* **205**, 357–363.

Heneka M. T., Galea E., Gavriluyk V., Dumitrescu-Ozimek L., Daeschner J., O'Banion M. K., Weinberg G., Klockgether T., Feinstein D. L. (2002) Noradrenergic depletion potentiates beta -amyloid-induced cortical inflammation: implications for Alzheimer's disease. *J. Neurosci. Off. J. Soc. Neurosci.* **22**, 2434–2442.

Heneka M. T., Gavrilyuk V., Landreth G. E., O'Banion M. K., Weinberg G., Feinstein D. L. (2003) Noradrenergic depletion increases inflammatory responses in brain: effects on IκB and HSP70 expression: PPARγ agonist reduce brain inflammatory responses. *J. Neurochem.* **85**, 387–398.

Heneka M. T., Nadrigny F., Regen T., Martinez-Hernandez A., Dumitrescu-Ozimek L., Terwel D., Jardanhazi-Kurutz D., et al. (2010) Locus ceruleus controls Alzheimer's disease pathology by modulating microglial functions through norepinephrine. *Proc. Natl. Acad. Sci.* **107**, 6058–6063.

Hoeijmakers L., Heinen Y., Dam A.-M. van, Lucassen P. J., Korosi A. (2016) Microglial Priming and Alzheimer's Disease: A Possible Role for (Early) Immune Challenges and Epigenetics? *Front. Hum. Neurosci.* **10**.

Holtmaat A., Bonhoeffer T., Chow D. K., Chuckowree J., De Paola V., Hofer S. B., Hübener M., et al. (2009) Long-term, high-resolution imaging in the mouse neocortex through a chronic cranial window. *Nat. Protoc.* **4**, 1128–1144.

Hulsey D. R., Hays S. A., Khodaparast N., Ruiz A., Das P., Rennaker R. L., Kilgard M. P. (2016) Reorganization of Motor Cortex by Vagus Nerve Stimulation Requires Cholinergic Innervation. *Brain Stimulat.* **9**, 174–181.

Hulsey D. R., Riley J. R., Loerwald K. W., Rennaker R. L., Kilgard M. P., Hays S. A. (2017) Parametric characterization of neural activity in the locus coeruleus in response to vagus nerve stimulation. *Exp. Neurol.* **289**, 21–30.

Jardanhazi-Kurutz D., Kummer M. P., Terwel D., Vogel K., Dyrks T., Thiele A., Heneka M. T. (2010) Induced LC degeneration in APP/PS1 transgenic mice accelerates early cerebral amyloidosis and cognitive deficits. *Neurochem. Int.* **57**, 375–382.

Jardanhazi-Kurutz D., Kummer M. P., Terwel D., Vogel K., Thiele A., Heneka M. T. (2011) Distinct adrenergic system changes and neuroinflammation in response to induced locus ceruleus degeneration in APP/PS1 transgenic mice. *Neuroscience* **176**, 396–407.

Kalinin S., Gavrilyuk V., Polak P. E., Vasser R., Zhao J., Heneka M. T., Feinstein D. L. (2007) Noradrenaline deficiency in brain increases beta-amyloid plaque burden in an animal model of Alzheimer's disease. *Neurobiol. Aging* **28**, 1206–1214.

Kandel E. R., ed (2013) *Principles of neural science*. McGraw-Hill, New York.

Krahl S. E., Clark K. B., Smith D. C., Browning R. A. (1998) Locus coeruleus lesions suppress the seizure-attenuating effects of vagus nerve stimulation. *Epilepsia* **39**, 709–714.

Lenth R. V. (2016) Least-Squares Means: The R Package lsmeans. *J. Stat. Softw.* **69**, 1–33.

Merrill C. A., Jonsson M. A. G., Minthon L., Ejnell H., C-son Silander H., Blennow K., Karlsson M., et al. (2006) Vagus nerve stimulation in patients with Alzheimer's disease: Additional follow-up results of a pilot study through 1 year. *J. Clin. Psychiatry* **67**, 1171–1178.

Miyamoto A., Wake H., Moorhouse A. J., Nabekura J. (2013) Microglia and synapse interactions: fine tuning neural circuits and candidate molecules. *Front. Cell. Neurosci.* **7**.

Mourao R. J., Mansur G., Malloy-Diniz L. F., Castro Costa E., Diniz B. S. (2016) Depressive symptoms increase the risk of progression to dementia in subjects with mild cognitive impairment: systematic review and meta-analysis. *Int. J. Geriatr. Psychiatry* **31**, 905–911.

Nichols J. A., Nichols A. R., Smirnakis S. M., Engineer N. D., Kilgard M. P., Atzori M. (2011) Vagus nerve stimulation modulates cortical synchrony and excitability through the activation of muscarinic receptors. *Neuroscience* **189**, 207–214.

O'Donnell J., Zeppenfeld D., McConnell E., Pena S., Nedergaard M. (2012) Norepinephrine: a neuromodulator that boosts the function of multiple cell types to optimize CNS performance. *Neurochem. Res.* **37**, 2496–2512.

Oshinsky M. L., Murphy A. L., Hekierski H., Cooper M., Simon B. J. (2014) Noninvasive vagus nerve stimulation as treatment for trigeminal allodynia. *Pain* **155**, 1037–1042.

Phillips C., Fahimi A., Das D., Mojabi F. S., Ponnusamy R., Salehi A. (2016) Noradrenergic System in Down Syndrome and Alzheimer's Disease A Target for Therapy. *Curr. Alzheimer Res.* **13**, 68–83.

Pinheiro J., Bates D., DebRoy S., Sarkar D., R Core Team (2017) *nlme: Linear and Nonlinear Mixed Effects Models*.

R Core Team (2016) *R: A Language and Environment for Statistical Computing*. R Foundation for Statistical Computing, Vienna, Austria.

Raedt R., Clinckers R., Mollet L., Vonck K., El Tahry R., Wyckhuys T., De Herdt V., et al. (2011) Increased hippocampal noradrenaline is a biomarker for efficacy of vagus nerve stimulation in a limbic seizure model. *J. Neurochem.* **117**, 461–469.

Ransohoff R. M. (2016) How neuroinflammation contributes to neurodegeneration. *Science* **353**, 777–783.

Roosevelt R. W., Smith D. C., Clough R. W., Jensen R. A., Browning R. A. (2006) Increased extracellular concentrations of norepinephrine in cortex and hippocampus following vagus nerve stimulation in the rat. *Brain Res.* **1119**, 124–132.

Rosas-Ballina M., Olofsson P. S., Ochani M., Valdés-Ferrer S. I., Levine Y. A., Reardon C., Tusche M. W., et al. (2011) Acetylcholine-synthesizing T cells relay neural signals in a vagus nerve circuit. *Science* **334**, 98–101.

Sjögren M. J. C., Hellström P. T. O., Jonsson M. A. G., Runnerstam M., Silander H. C.-S., Ben-Menachem E. (2002) Cognition-enhancing effect of vagus nerve stimulation in patients with Alzheimer's disease: a pilot study. *J. Clin. Psychiatry* **63**, 972–980.

Smiley J. F., Subramanian M., Mesulam M. M. (1999) Monoaminergic-cholinergic interactions in the primate basal forebrain. *Neuroscience* **93**, 817–829.

Tynan R. J., Weidenhofer J., Hinwood M., Cairns M. J., Day T. A., Walker F. R. (2012) A comparative examination of the anti-inflammatory effects of SSRI and SNRI antidepressants on LPS stimulated microglia. *Brain. Behav. Immun.* **26**, 469–479.

Vida G., Peña G., Kanashiro A., Thompson-Bonilla M. del R., Palange D., Deitch E. A., Ulloa L. (2011) β2-Adrenoreceptors of regulatory lymphocytes are essential for vagal neuromodulation of the innate immune system. *FASEB J. Off. Publ. Fed. Am. Soc. Exp. Biol.* **25**, 4476–4485.

Vonck K., Raedt R., Naulaerts J., De Vogelaere F., Thiery E., Van Roost D., Aldenkamp B., Miatton M., Boon P. (2014) Vagus nerve stimulation…25 years later! What do we know about the effects on cognition? *Neurosci. Biobehav. Rev.* **45**, 63–71.

Yakunina N., Kim S. S., Nam E.-C. (2017) Optimization of Transcutaneous Vagus Nerve Stimulation Using Functional MRI. *Neuromodulation J. Int. Neuromodulation Soc.* **20**, 290–300.

Zarow C., Lyness S. A., Mortimer J. A., Chui H. C. (2003) Neuronal loss is greater in the locus coeruleus than nucleus basalis and substantia nigra in Alzheimer and Parkinson diseases. *Arch. Neurol.* **60**, 337–341.

Zhang Q., Lu Y., Bian H., Guo L., Zhu H. (2017) Activation of the α7 nicotinic receptor promotes lipopolysaccharide-induced conversion of M1 microglia to M2. *Am. J. Transl. Res.* **9**, 971–985.

Figure Legends

Figure 1

Linear trend analysis for **12-month-old** mice groups. 3D microglia reconstructions in APP/PS1 (A) and WT (B) animals before (Prestim), 40 minutes and 80 minutes after nVNS or sham-treatment. Normalised observed data are represented by the continuous lines in blue (nVNS) and orange (sham-treatment), the linear regression is represented by the dotted lines. The response variables are number of branches (C), total branch length (D) and average branch order (E). Slope comparison between nVNS and sham-treatment (F, G, H). The data show a significant time-dependent difference between nVNS and sham-treatment for the number of branches ($p < 0.0001$ ***) and total branch length ($p = 0.0028$ **) in APP/PS1 mice and a non-significant trend for number of branches ($p = 0.071$) and total branch length ($p = 0.0911$) in WT animals. A significant time-dependent change between nVNS and sham-treatment was seen in the average branch order ($p = 0.0497$) for WT animals and a non-significant trend ($p = 0.0897$) for APP/PS1 mice. P-values and confidence intervals are adjusted using multivariate testing method (mvt) for 4 estimates. 95% CI (C, D, E) and SEM + 95% CI (F, G, H). n.s. $p >= 0.05$, * $p < 0.05$, ** $p < 0.01$, *** $p < 0.001$. The APP/PS1 and WT mice ($n = 20$) are divided in stimulated ($n = 3$) and sham-treated mice ($n = 2$) with a total of $n = 469$ cells.

Figure 2

Interaction scheme between microglia and non-invasive vagus nerve stimulation (nVNS). Stimulation of the Locus coeruleus (LC) and the Nucleus Basalis of Meynert (NBM) following nVNS leads to activation of the cholinergic (CAP) and the noradrenergic (NAP) anti-inflammatory pathways. The LC fibers lead widely throughout the brain to areas like the NBM, Hippocampus and the cerebral cortex. The most prevalent neurotransmitters here are Norepinephrine (NE) and Acetylcholine (ACh). The suggested target on microglia cells for ACh is the α7nAChR, whereas NE mainly activates β1 and β2 receptors. The activation of these pathways is associated with a general anti-inflammatory response.

Healthy microglia have better Aβ phagocytosis capabilities and increased release of neurotrophic factors (BDNF, bFGF) and anti-inflammatory cytokines (IL-4, IL-10, TNFβ). These surveying microglia (represented on the left side of the figure in blue) which typically show long, ramified branches also help pruning of neuronal synapses.

During aging, and even more in addition to external (infections, acute traumata) or internal (Aβ deposition, stress, depression) stimuli, microglia cells get primed or even chronically activated. This leads to neuroinflammation and a toxic environment in which pro-inflammatory cytokines (IL1-β, IL-6, TNFα) of the now ameboid cells with retracted processes get released (represented on the right side of the figure in red).

This pro-inflammatory environment can lead to extensive neuronal loss and in the end dementia.

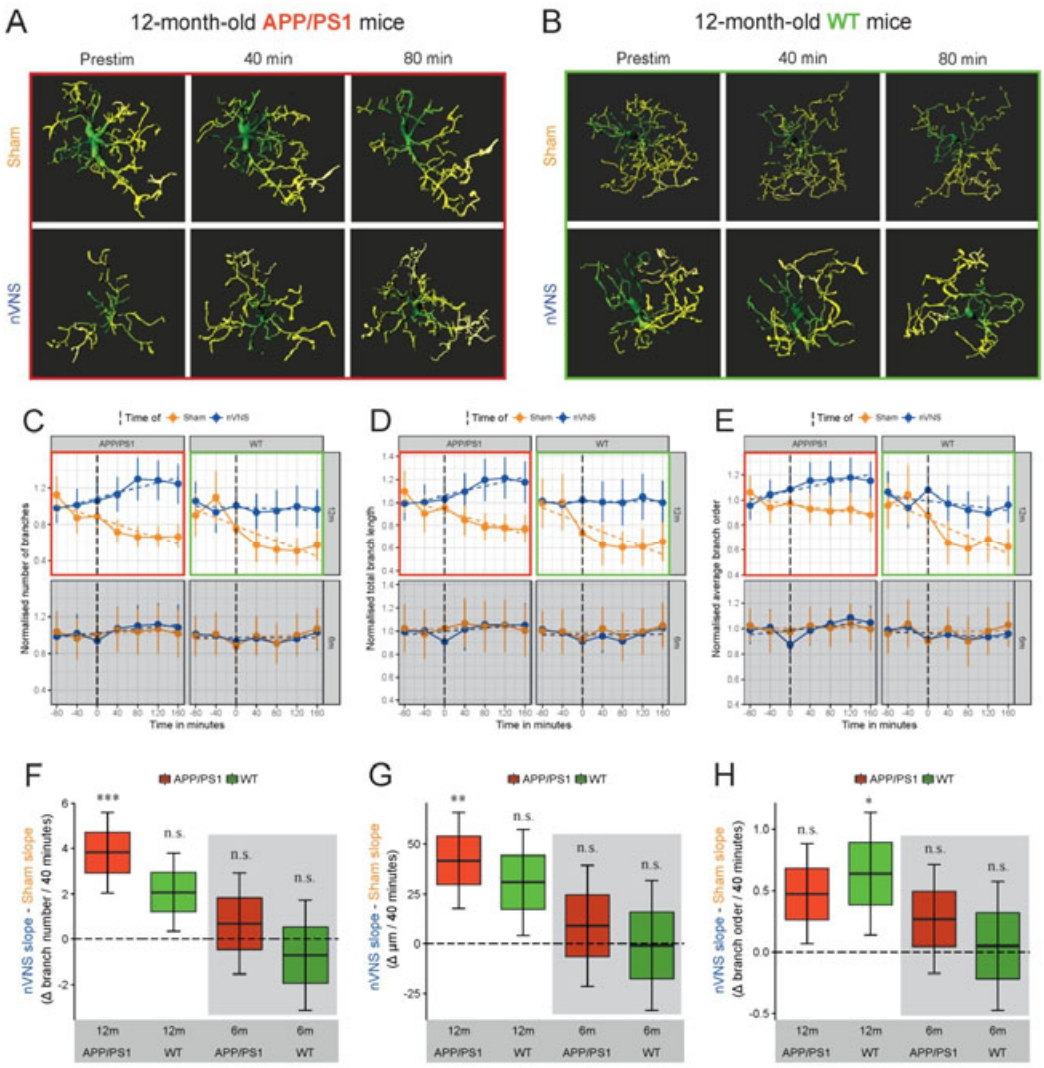

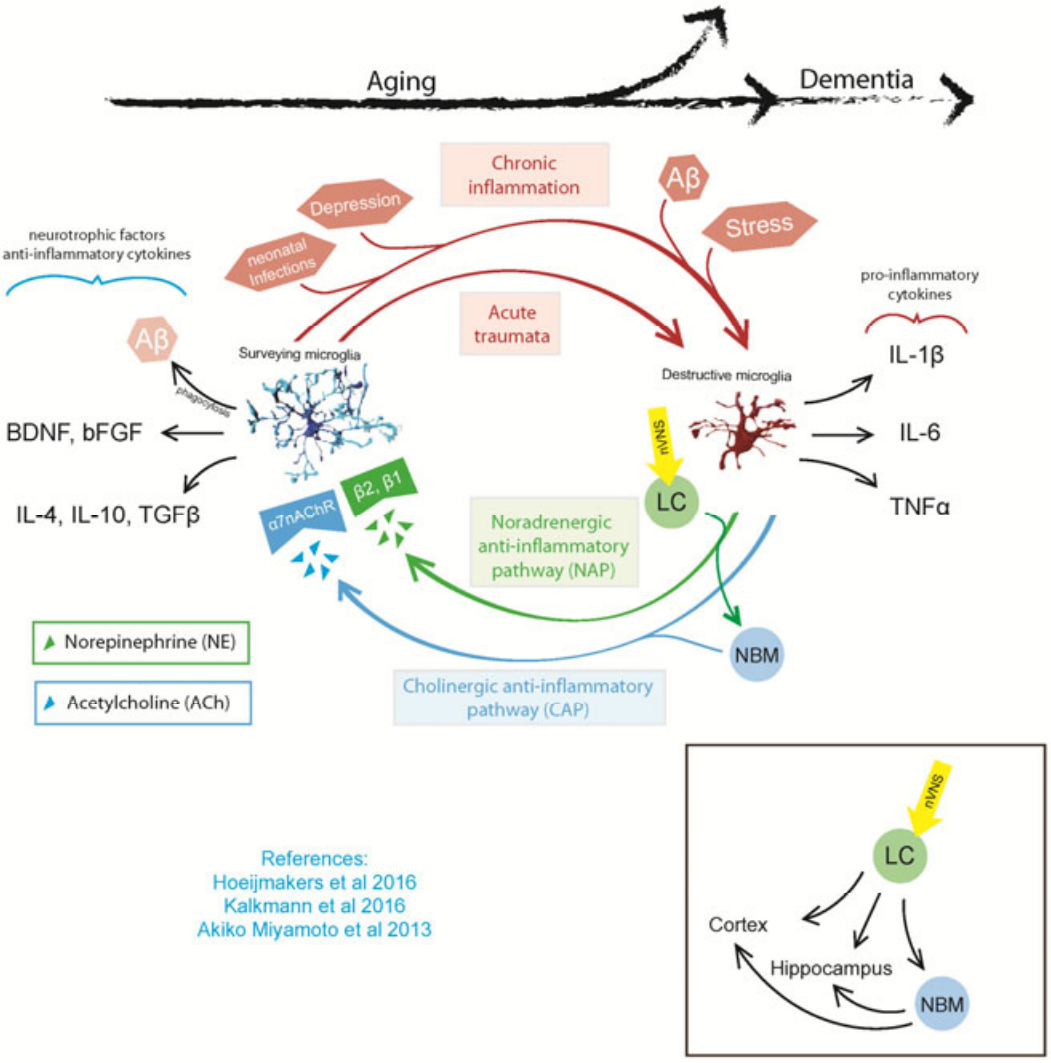

References:
Hoeijmakers et al 2016
Kalkmann et al 2016
Akiko Miyamoto et al 2013